Optik - International Journal for Light and Electron Optics 278 (2023) 170701

Contents lists available at ScienceDirect

Optik - International Journal for Light and Electron Optics

journal homepage: www.elsevier.com/locate/ijleo

Original research article

Asymmetric hybrid full-duplex POF-based VLC transmission links

Juan Andrés Apolo [a,*], Shivani Rajendra Teli [b], Carlos Guerra-Yánez [b], Vicenç Almenar [a], Beatriz Ortega [a], Stanislav Zvánovec [b]

[a] Instituto de Telecomunicaciones y Aplicaciones Multimedia (ITEAM), Universitat Politecnica de Valencia, Camino de Vera s/n, Valencia, 46022, Spain

[b] Faculty of Electrical Engineering, Czech Technical University in Prague, Dejvice-Praha 6, Prague, 16627, Czech Republic

ARTICLE INFO

Keywords:
Optical wireless communications
Visible light communications
Optical camera communications
Polymer optical fiber
Full-duplex

ABSTRACT

This paper presents an asymmetric full-duplex solution based on visible light communications (VLC) for indoor wired and wireless hybrid signal transmission. The signal is distributed by a polymer optical fiber (POF) link and passively radiated. The proposed system includes two VLC links: a low-speed downlink and a high-speed uplink using an image sensor (IS) and photodiode detection (PD) based receivers. PD-based system communication performance is evaluated by means of error vector magnitude (EVM) for different modulation orders quadrature phase shift keying (QPSK), 16- and 64-quadrature amplitude modulation (QAM), while the IS-based system is characterized in terms of the success of reception (SoR). High-speed data transmission up to 160 Mbps with a 16-QAM modulation scheme and low-speed data transmission up to 500 bps with 98.6% of SoR using a non-return zero on–off keying (NRZ-OOK) scheme over a 1.5 m optical wireless link are demonstrated. Finally, simulations of the wireless channel are performed to evaluate the misalignment tolerance of the system; and, to estimate the uplink performance at longer distances.

1. Introduction

Optical wireless communications (OWC) have aroused significant industry and academic interest. Particularly, visible light communications (VLC), optical camera communications (OCC) and free-space optical (FSO) communications over infrared (IR) are emerging technologies. They have become alternatives to traditional radio frequency (RF) communications due to the availability of a large portion of additional unlicensed spectrum to satisfy the growing requirements for Internet access and multimedia services [1].

Light-emitting diodes (LEDs) are employed as optical transmitters in VLC systems thanks to their low power consumption, free spectrum license, high security and long lifetime in spite of their typical limited bandwidth, e.g. 20 MHz [2]. These features enable VLC to be cost-effectively and easily integrated into existing lighting systems. After the first standard was published by the Wireless Personal Area Networks (WPANs) IEEE working group in 2011 [3], VLC has emerged as a fast-growing technology for various scenarios, as well as in numerous research studies [4,5]. Regarding applications, VLC may be integrated to build a wireless small-cell access network, where multiple light sources are used as access points (APs) in indoor environments [6], for underwater communication systems [7], for positioning systems, or intelligent transportation systems (ITS) as vehicle-to-vehicle communication [8] or data transmission via traffic lights and vehicle LEDs [9]. Furthermore, recent works have demonstrated the use of hybrid networks using plastic optical fiber (POF) and VLC for indoor optical communications [10,11]. The advantages of POF

* Corresponding author.
E-mail addresses: juaapgon@teleco.upv.es (J.A. Apolo), telishiv@fel.cvut.cz (S.R. Teli), guerrcar@fel.cvut.cz (C. Guerra-Yánez), valmenar@dcom.upv.es (V. Almenar), bortega@dcom.upv.es (B. Ortega), xzvanove@fel.cvut.cz (S. Zvánovec).

https://doi.org/10.1016/j.ijleo.2023.170701
Received 19 August 2022; Received in revised form 1 February 2023; Accepted 17 February 2023
Available online 21 February 2023

are large core diameter, small bending radius and lightweight resulting in low cost and easy solution to integrate end-user access into the edge network through an optical backbone [12].

As an extension of the previous Short-Range OWC IEEE standard, optical camera communications (OCC) was included in IEEE 802.15.7-2018 [13], where the receivers are digital cameras with a lens and an image sensor (IS). In recent years, in spite of the low bit rate, the integration of IS, or optical cameras, in smartphones has massively increased, and opportunities are emerging for OCC to address multiple challenges in different applications such as the Internet of Things (IoT), indoor localization [14], motion capture and intelligent transportation systems. Examples of them represent safety-related applications such as accident notifications, detecting and recognizing moving vehicles, collision warnings, pedestrian detection, range estimation of approaching vehicles, and information related to speed and direction [15]. Most of cameras make use of a Complementary Metal–Oxide–Semiconductor (CMOS) IS. Note that OCC is limited to low bit data rates (kbps) due to the receiver sampling rate, determined by the camera's frame rate, typically in the range of 30 to 60 frames per second (fps) [16]. However, the rolling shutter effect of the CMOS sensors, which sequentially (row by row) integrates the light illuminating the pixels and does not capture the image at once, is used to increase the bit rate (R_b) and achieve flicker-free communication [17].

VLC also provides a promising infrastructure for IoT applications, not only for mainstream consumer applications, but also for industrial and Industry 4.0, where smart devices (sensors, actuators, machines and robots) send wireless data over flexible networks to perform a real-time industrial control using minimal human intervention with reduced costs [18]. However, most of the research efforts done towards the development of VLC technology have been focused on optimizing communication throughput over a one-way channel, mainly the downlink. The establishment of bidirectional communication is highly desirable, although for the uplink, the use of VLC may not always be the optimum choice. Note that power constraint on devices, alignment and line-of-sight (LOS) from transmitters (Tx) to receivers (Rx) and interference due to reflections between uplink and downlink channels are all important issues to consider in order to obtain a proper performance of the system [19]. The definition of the optimal technology for the uplink depends upon the scenario requirements; for example, in an industrial environment where a built-in robot camera may capture images or videos, this camera can also receive short signaling messages while the uplink is used to transmit high-speed data (e.g. video) to the factory core network over an asymmetrical full-duplex link.

In VLC, two methods support bidirectionality while avoiding crosstalk due to signal reflections: wavelength division duplexing (WDD) and time division duplexing (TDD). In [20], for example, a VLC-IoT wireless communication system based on a non-orthogonal multiple access technique while using visible spectrum in downlink and IR for uplink is proposed, although IR eye safety must be ensured by limiting the transmission power. A full-duplex link using LEDs in the visible band for both directions has also been reported, but low data rates (several kbps) and short transmission distances (several cm) were achieved [21]. Researchers in [22] addressed bidirectionality in a TDD-based scheme for multiple users. Both uplink and downlink were performed over the same wavelength. Tests were carried out with commercial illumination LEDs over a 3 m long wireless link, achieving speeds up to 100 Mbps. In [23], the authors present a full-duplex VLC system using POF for remote signal distribution in indoor environments. They present a WDM scheme for establishing multiple access points for the users with a coverage radius of about 30 cm for a 1.2 m wireless link and the achieved speeds were 2 Gbps for the uplink and downlink. In contrast to our work, the uplink and downlink were based on VLC channels employing photodiodes as receivers and laser diodes as transmitters.

This work provides a full-duplex communication solution in an asymmetric scenario using VLC technology based on PD for uplink and IS for downlink. In particular, we consider a low-speed link IS-based, transmitting on–off keying (OOK) baseband signal and a high-speed rate M-order quadrature amplitude modulation (QAM) signal transmission based on PD, while using POF for the passive distribution of the signals. The main contributions of this work can be summarized as follows:

(1) A hybrid POF/VLC network is developed using VLC technology to support bidirectional WDD-based communication services.
(2) A full-duplex asymmetric VLC link is demonstrated. A high-speed M-QAM signal is transmitted using the PD-based uplink and a low-speed baseband signal is transmitted using the IS-based downlink.
(3) Passive wired to wireless interface with commercial off-the-shelf components is employed where a single lens transmits and receives light from both communication channels.
(4) Using a passive POF network for signal distribution simplifies the optical network infrastructure supporting multiple APs, i.e. it creates an all-optical backhauling with no intermediate electrical conversions and enables the connection of end users to the core network.
(5) Simulations of the optical channels are performed to extend the results and evaluate the tolerance of the system to misalignment, as well as to provide the maximum experimental bit rates in terms of wireless link distance.

The remaining sections of this document are organized as follows: Section 2 presents the description of the hybrid VLC full-duplex link. Section 3 provides and discusses the experimental results, in Section 4, an optical simulation of the system is employed to characterize the proposed solution, and Section 5 summarizes the main conclusions of this paper.

2. Description of hybrid VLC/OCC full-duplex link

This part provides the description and characteristics of the implemented full-duplex system. Fig. 1(a) shows the hybrid VLC full-duplex asymmetric link scheme for an indoor point-to-point transmission scenario based on LEDs as transmitters while a photograph of the laboratory setup is shown in Fig. 1(b) . The system combines: (i) a low-speed VLC link using a camera as a detector for UL, and (ii) a high-speed VLC link using a PD as a detector for downlink.

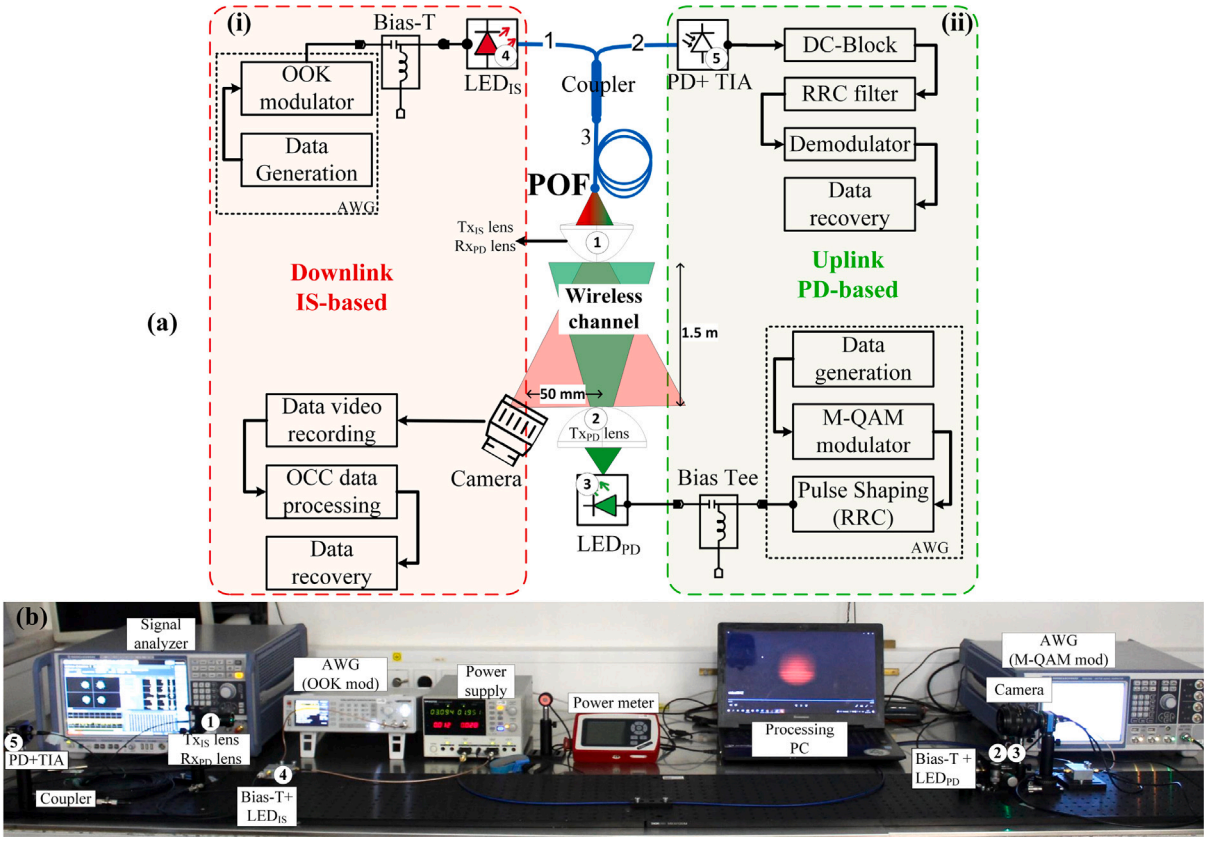

Fig. 1. (a) Scheme of the proposed approach for full-duplex VLC transmission. Insets: (i) IS-based downlink, (ii) PD-based uplink; (b) Photograph of the laboratory setup. PD (photodiode), TIA (transimpedance amplifier), AWG (Arbitrary Waveform Generator), OOK (On–Off-Keying), POF (plastic optical fiber), Tx (transmitter), Rx (receiver), RRC (root-raised-cosine).

The optical signal is distributed through a Step-Index (SI)-POF; thus, both the transmitter of the IS-based downlink and the receiver of the PD-based uplink can be placed remotely. Furthermore, the optical network infrastructure is simplified, as the optical frontend is passive and includes a unique lens operating as a transmitting and receiving lens for the IS- and PD-based link, respectively. A POF optical 2 × 1 coupler is used to combine these two signals in one fiber, i.e. LED$_{IS}$ output is launched into port#1, while port#3 connects the POF that distributes the signal and port#2 collects the signal back to the high-speed link receiver. Note that both links can be exchanged, i.e., photodetector for downlink and cameras for uplink, but in this case, OCC could not make use of the POF signal distribution.

2.1. Hybrid POF and IS-based downlink

The transmitter consists of a commercial red LED (see ④ in Fig. 1, Avago SFH757V) emitting the optical carrier signal centered at $\lambda = 650$ nm that is launched into the POF through a 1 mm diameter POF connector. A non-return-to-zero and on–off-keying (NRZ-OOK) modulation is employed. An arbitrary waveform generator (R&S HMF2550) is used to generate the data signal and directly modulate the light intensity of the LED$_{IS}$ by using a bias-T (BT-A11). A bias current of 48 mA is applied with an output optical power of 0 dBm. The modulated light beam is launched into a 1 mm diameter and 1 m long SI-POF (i.e. POF radius $r_{POF} = 0.5$ mm) through a POF coupler, with the POF end coupled to an aspheric lens ACL25416U (see ① in Fig. 1) from Thorlabs with focal length $f_{①} = 16$ mm to create the wireless channel interface of 1.5 m long. The key characteristics of the elements composing both communication links are summarized in Table 1.

A CMOS rolling-shutter based camera (DFK 72BUC02) is used on the Rx side, which in rolling-shutter acquisition mode scans the whole image row by row of pixels using a delay between each row. So, the camera sequentially integrates all the illuminated pixels during the exposure time. In a single captured image, the rolling-shutter scheme allows multiple exposures, which allows multiple incoming light states to be captured simultaneously within a single frame, as each row is exposed once to light. This scheme allows for flicker-free communication and bit rate enhancement. The camera is configured to capture a video stream of 25 fps; a resolution of 648 × 484 (red–green–blue, RGB); and an exposure time of 25 μs while the gain is set between 4–8 dB [24].

Table 1
Main configuration parameters of the VLC full-duplex link.

Parameter		Value
IS-based downlink		
LED_{IS}	Avago SFH757V	
	Bias current	48 mA
	λ_{peak}	650 nm
	V_{bias}	1.9 V
	Optical power	0 dBm
Camera	DFK 72BUC02	
	Resolution	648 × 484 pixels
	Frames	25 fps
	Exposure	200 μs
	Gain	4.8 dB
PD-based uplink		
LED_{PD}	Vishay VLMTG1501-GS08	
	Bias current	11 mA
	λ_{peak}	6535 nm
	V_{bias}	3.1 V
	Optical power	6.4 dBm
PD	PDA10A	
	Wavelength range	200 nm to 1100 nm
	Bandwidth	150 MHz
	Active area	∅1 mm (0.8 mm^2)
	Peak responsivity	0.44 A/W λ_{peak} = 730 nm
General		
Tx_{PD} lens	Thorlabs LA1951-A	
	Diameter	1″
	Focal length	25.3 mm
Rx_{PD} lens Tx_{IS} lens	Thorlabs ACL25416U-A	
	Diameter	1″
	Focal length	16 mm
POF	Diameter	1″
	Profile	Step-Index (SI)
	Material	PMMA
General	Wireless link	1.5 m
	POF length	1, 20 m

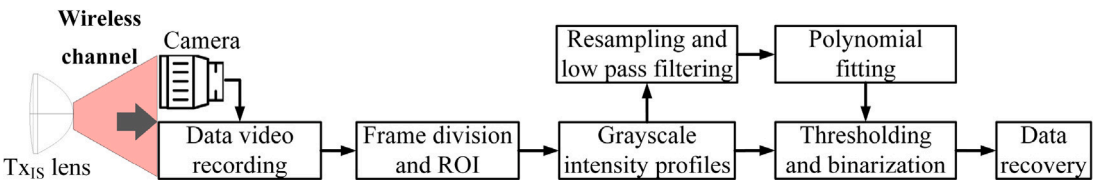

Fig. 2. Block diagram of IS-based downlink including data signal processing.

The transmitted data packet is composed of a 7-bit data sequence [0 0 1 1 0 1 1]. The camera output signal is captured for subsequent offline data processing in Matlab based on traditional image processing (see Fig. 2). The captured signal, a video stream, is divided into image frames for further frame-by-frame processing to decode the received data. Then, a processing module is applied to find the region of interest (ROI) where the LED_{IS} light is located into the image. The images are then converted from RGB to grayscale to retrieve the intensity profiles. After that, a second-order polynomial fitting technique (as described in [25]) is applied to mitigate the interferometric nature observed due to the ambient light in the surrounding. The grayscale intensity profiles after fitting are normalized for thresholding and binarization of data frames and converted to a vector transformation for decoding the data bit streams.

2.2. Hybrid POF and PD-based uplink

The Tx_{PD} consists of a commercial green Chip LED (see ③ in Fig. 1, Vishay VLMTG1501-GS08), emitting an optical carrier signal centered at a wavelength λ = 520 nm. An arbitrary waveform generator (R&S, SMW200 A) is employed to generate the data

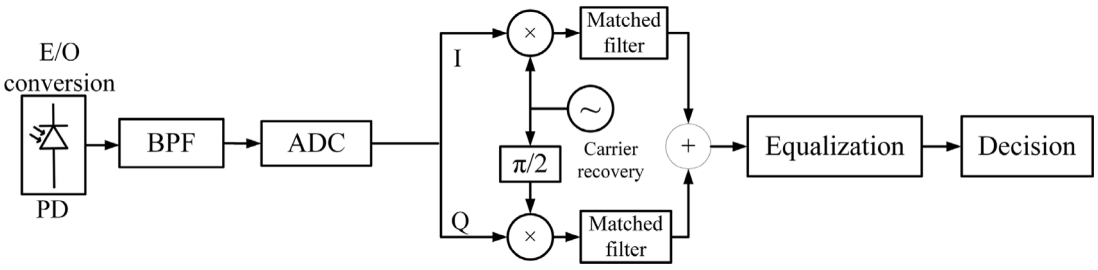

Fig. 3. Simplified block diagram of M-QAM signal data processing. O/E (Opto-Electric). BPF (Band-pass filter), ADC (Analog-to-digital converter).

Table 2
Power budget.

Description	Unit	PD-based uplink	IS-based downlink
Optical power at LED	dBm	6.3	0
Coupling losses (lens)	dB	7.1	0.6
Wireless channel (1.5 m)	dB	8.8	11.0
Insertion losses (coupler)	dB	5.9	4.2
Polymer optical fiber (1 m)	dB	0.2	0.2
Connectors + misalignment errors	dB	3.5	3.5
Received optical power at the detector	**dBm**	**−19.2**	**−19.5**

signal, which is directly applied to modulate the intensity of the LED_{PD} by using a bias-T (BT-A11). The LED_{PD} emits an optical power of 6.4 dBm with a bias current of 11 mA (V_{bias} = 3.1 V). In particular, quadrature phase shift keying (QPSK), 16 and 64-QAM modulation formats are used over the carrier frequencies of 50 MHz, 40 MHz and 20 MHz, respectively, employing a square-root raised-cosine (RCC) pulse shaping with a roll-off factor of 0.25. Next, a Thorlabs LA1951 spherical lens (see ② in Fig. 1) with a focal length $f_{②}$ = 25 mm is used to create the wireless channel interface of 1.5 m long as the one shown in [26]. The same lens from the IS-based downlink is used on the receiver side to focus the beam into an SI-POF 1 m section (see ① in Fig. 1). A 2 × 1 POF optical coupler is then used to guide the light into a 1 mm diameter PD (see ⑤ in Fig. 1, Thorlabs PDA10 A) incorporating a fixed-gain trans-impedance-amplifier (TIA). Finally, the data signal is captured and demodulated using typical QAM demodulation blocks (see Fig. 3) by a digital signal analyzer (R&S, FSW26).

By default, it is assumed that the I/Q data is modulated at one of the carrier frequencies mentioned above. An antialiasing band-pass filter (BPF) is applied before the analog-to-digital converter (ADC) that captures the received signal. Next, the digital signal is down-converted to baseband and matched-filtered with a root raised-cosine filter to remove noise and high-frequency terms. Finally, an equalizer compensates for channel distortion, and symbols are de-mapped to recover the original information bits.

2.3. Power budget

Table 2 summarizes the power budget of both links. The coupling losses between the LED_{PD} and the Tx_{PD} lens are particularly high for the PD-based uplink, as explained in the following. The half-intensity angle of the LED_{PD} is ±65 degrees and corresponds to a Lambertian radiation pattern. The numerical aperture (NA) of the Tx_{PD} lens is 0.5, equivalent to a light acceptance cone below 30 degrees. On the other hand, for the IS-based downlink, the coupling losses are 0.6 dB as the LED_{IS} package includes a molded micro-lens for efficient coupling. The difference in the propagation losses of the optical channel is due to both the geometry of the lenses of each particular system and the positioning of the lenses in the system. Compared to the PD-based uplink, the source and lens combination generates a beam with higher divergence in the IS-based downlink. In addition, the receiving lenses on each link have different diameters, and therefore their gain differs. The details are discussed in Section 4. Note that the insertion losses between the ports of the 2 × 1 directional coupler are not identical.

3. Full-duplex transmission measurements

As explained in the previous section, the proposed system includes two VLC links operating simultaneously: the PD-based uplink for high-speed data channels and the IS-based downlink for low-speed data channels. The last one uses a baseband modulation whose bandwidth is widely separated from the RF bandwidth used for the PD-based uplink to avoid interference between both channels. Furthermore, in the optical domain, the directivity of the coupler between the IS- and PD-based signals is 20.7 dB. Consequently, the PD is not saturated by the IS-based signal and crosstalk at the PD is reduced. In the IS-based downlink, any reflection of the PD-based signal is detected by the camera as a constant light level due to the low-pass filter effect; these reflections modify the luminance of the received pixels, increase the noise level and can cause errors in the decoding process. Therefore, in this case, it is necessary to add an optical filter, which can be done by software since the RGB camera allows color filtering, and thus, no additional hardware is required. The laboratory measurements are carried out with both links running simultaneously.

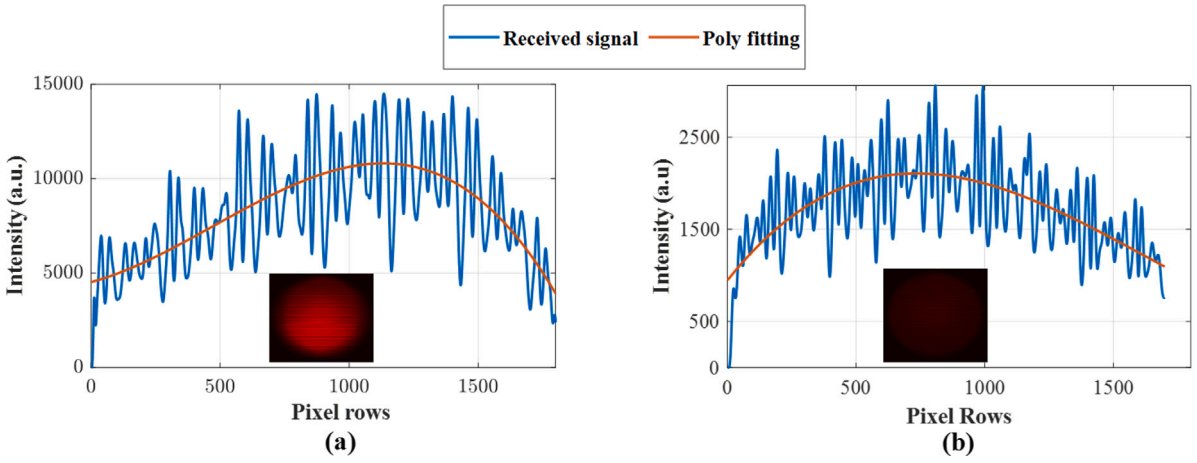

Fig. 4. Experimental grayscale values of the received data for 500 bps, 4 dB of camera gain: (a) 1.5 m; and, (b) 3.5 m wireless link. Insets show a captured frame.

Table 3
IS-based system performance summary.

	Bit rate (bps)	Gain (dB)	Wireless channel span (m)				
			1.5	2	2.5	3	3.5
Success of reception (%)	500	4	98.6	92.8	92.9	87.1	84.3
		8	95.7	90.0	88.6	88.6	78.6
	1000	4	62.9	61.4	60.0	60.0	58.6
		8	60.0	60.0	58.0	58.0	55.7

3.1. Downlink channel (IS-based VLC downlink)

The performance of the downlink channel is evaluated in terms of the success of reception (SoR). The SoR is the ratio of the correctly decoded against the total number of transmitted bits. In a line-of-sight OCC system, the bit rate is also conditioned by the projection size of the optical beam at the IS (ROI), since this projection contains the transmitted data bits in the received frames. A non-uniform illumination pattern of the optical source produces a non-uniform intensity profile. In our system, the Lambertian radiation pattern of the LED_{IS} produces a high-intensity profile in the center of the frame and a gradual decrease at the edges (see Fig. 4). This effect creates an SNR disparity in the frame, i.e. the SNR is non-uniform and is higher at the center region, thus hindering the demodulation process. A polynomial fitting method is applied to reduce the impact of non-uniform SNR, as described in [25]. Fig. 3 shows the difference in the intensity profile caused by the optical power level at different wireless link distances, 1.5 m(a) and 3.5 m(b) while insets display the captured frames.

Table 3 summarizes the performance results of the downlink channel using the SoR metric as a function of: (i) OCC signal transmission rate (500, 1000 bps); (ii) camera gain values (4, 8 dB) and (iii) different transmission distances (1.5–3.5 m). It can be observed the SoR was above 88% at bit rate of 500 bps and gain of 8 dB for transmission span of up to 3 m. Note, the success of reception is higher at lower bit rate due to limited camera bandwidth (25 fps) and reduces to 58% at the bit rate of 1000 bps. This is mainly due to the reduction in the pixel occupancy on the image frame with increase in bit rate. Similarly, increase in gain amplifies the noise and reflections from the fiber in terms of attenuation. Therefore, the performance of the OCC link degrades with increase in the camera gain values.

3.2. Uplink channel (PD-based VLC)

PD-based uplink performance is analyzed by measuring the error vector magnitude (EVM) to estimate the SNR at the receiver [27], this estimation is accurate if the main distortion at the receiver is caused by additive white Gaussian noise. At the reception, we set a target BER of 10^{-3} as it can be converted in an error-free transmission if forward error correction (FEC) is employed [28]. For each QAM modulation order, this target BER is related to a different SNR and its corresponding EVM [27]. In our measurements, QPSK, 16-QAM and 64-QAM are employed, and their corresponding EVM thresholds must be lower than 32.5%, 15% and 7.5%, respectively, to attain error-free transmission.

The EVM was measured as a function of the transmitted modulation bandwidth to test the feasibility of the approach and to evaluate the maximum achievable capacity under different conditions. Fig. 5 shows the transmission results for three modulation formats, i.e. QPSK, 16 and 64-QAM, which have been measured using two different POF lengths: 1 m and 20 m. According to Table 2, the received optical power (RoP) at the detector for 1 m POF is -19.2 dBm but RoP of -22.2 dBm was measured for 20 m

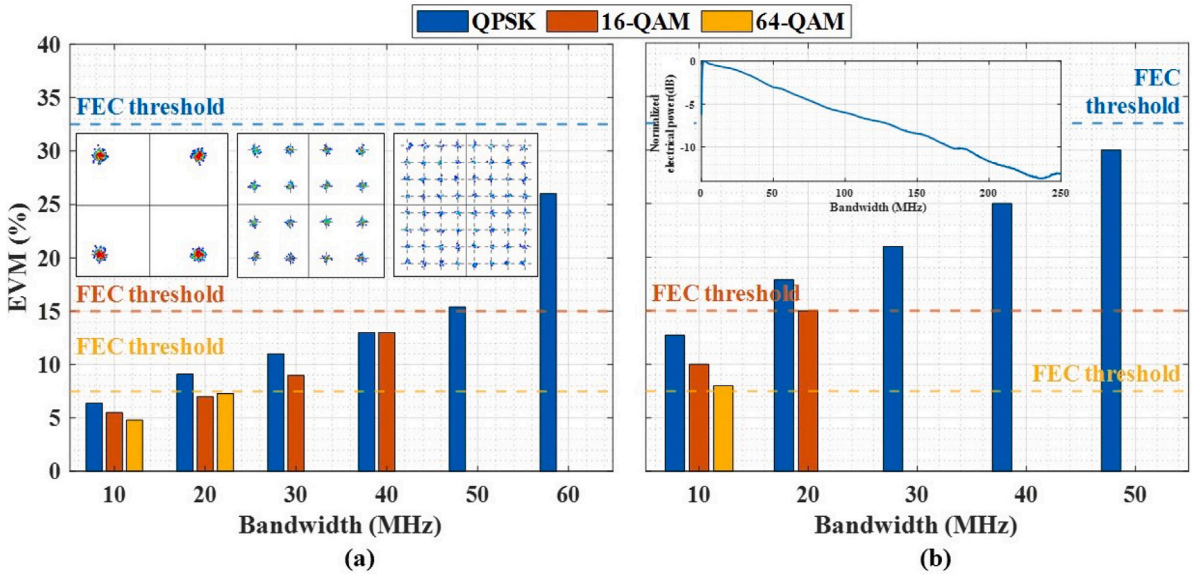

Fig. 5. EVM measurements for different modulation formats QPSK, 16 and 64 -QAM transmitted over different POF lengths: (a) 1 m (inset shows constellations obtained for 10 MHz bandwidth signals); (b) 20 m (inset shows the electrical frequency response of the PD-based OB2B link).

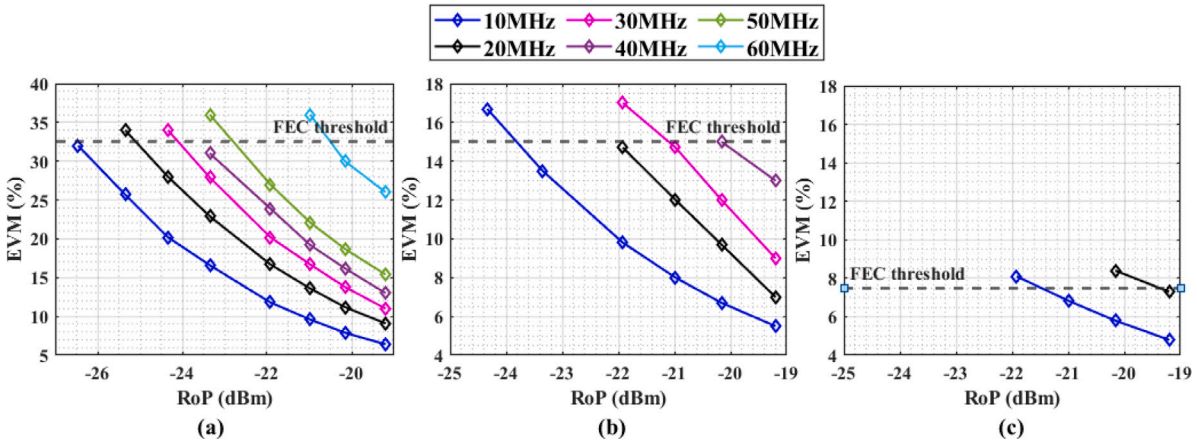

Fig. 6. EVM measurements as a function of RoP for signals with different bandwidth: (a) QPSK; (b) 16-QAM; and (c) 64-QAM.

POF. The modulation bandwidths satisfying the EVM FEC thresholds have been estimated in the former case to be around 60 MHz, 40 MHz and 20 MHz; while in the latter, 50 MHz, 20 MHz and 10 MHz are obtained. Note that, different maximum bandwidths are supported for different modulation formats for a given RoP value since the corresponding EVM thresholds are related to the required SNR. In addition, the insets in Fig. 5(a) show the measured constellation of signals with 10 MHz bandwidth for different modulation schemes transmitted through 1.5 m wireless link and 1 m POF. The inset in Fig. 5(b) shows the frequency response of the optical Back-to-Back (OB2B) link, whose 3 dB bandwidth can be estimated as 50 MHz.

EVM measurements for different bandwidths and modulation formats as a function of RoP are shown in Fig. 6. To adjust the RoP at the detector, neutral density absorbing filters from 0.1 to 0.7 optical density (Thorlabs NExxB) were used. RoP was measured using an S120C photodiode power sensor and a PM100D console. In particular, the measurements show that a minimum RoP of -26.5 dBm, -23.8 dBm, and -21.4 dBm are required to transmit a 10 MHz bandwidth signal for QPSK, 16- and 64-QAM, respectively. It can also be observed that a RoP penalty of about 1.5 dB exists for a fixed EVM when the modulation bandwidth is doubled, which corresponds to a difference of 3 dB in terms of received electrical power (ReP). This penalty is maintained up to 50 MHz of bandwidth and occurs when the bandwidth is doubled as a consequence of doubling the noise power. For 60 MHz, the penalty increases due to distortions introduced by the optical source (see inset Fig. 5(b)), which cannot be compensated by the equalizer.

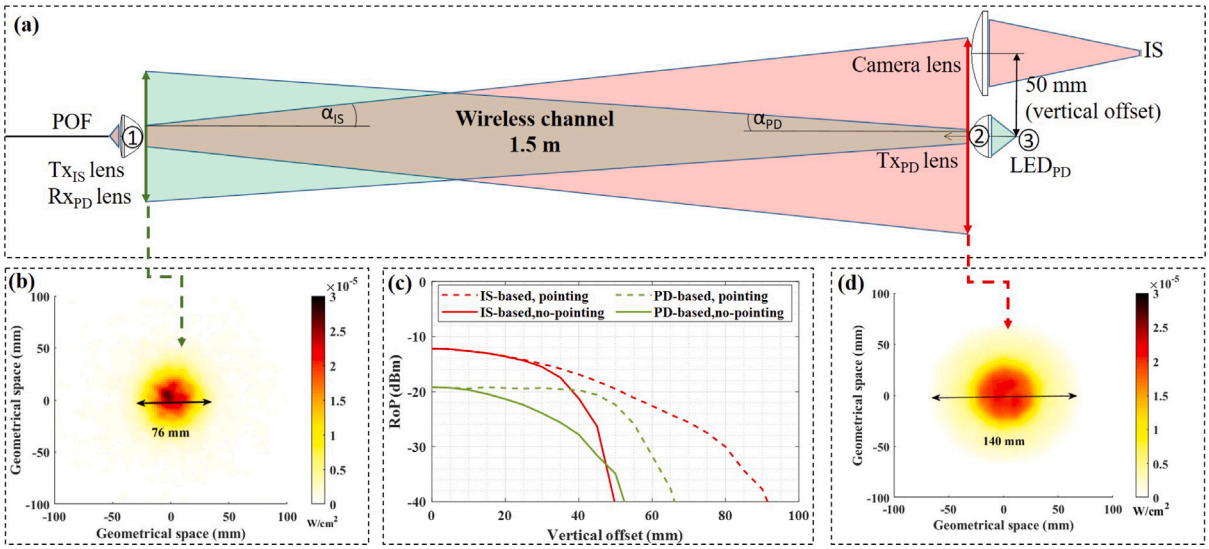

Fig. 7. System simulation results: (a) Full-duplex system simulation schematic, (b) Transversal section of the optical beam for the PD-based system after 1.5 m of the wireless link, (c) RoP as a function of vertical displacement of: Tx_{PD} (green); and Tx_{IS} (red), (d) Transversal section of the optical beam for the IS-based system after 1.5 m of the wireless link. (For interpretation of the references to color in this figure legend, the reader is referred to the web version of this article.)

4. Full-duplex link optical simulation

Simulations are carried out to complement the experimental results for the sake of evaluating the system tolerance to misalignment and providing achievable maximum bit rates of the PD-based uplink as a function of wireless link distance. The simulation setup depicted in Fig. 7(a) is employed to evaluate the system tolerance to misalignment: the Tx_{PD} lens is perfectly aligned to the Rx_{PD} lens while the camera lens has a 50 mm offset from the center of the Tx_{PD} lens, the wireless link distance of 1.5 m corresponds to the laboratory setup. The system is modeled and simulated using Zemax software in non-sequential mode, using the parameters detailed in the previous sections. Optical elements are configured using the manufacturers' specifications, while the software employs both a large number of rays and power spectral density to model the optical source.

Fig. 7(b) and (d) show the beam diameter for the PD- and IS-based link, respectively. The beam size is conditioned by its diameter at the lens output, its divergence and the distance at which it is measured. The divergence is given by $\alpha_{IS} = r_{POF}/(f_{①})$, i.e., the smaller the optical source and the longer the focal length, the smaller the divergence and hence the smaller the diameter of the light beam. For the PD-based uplink, the diameter is approximately 76 mm, while for the IS-based downlink, it is approximately 140 mm. Another parameter to evaluate the system misalignment is the receiver's angular field of view (AFOV), defined as the full angle (in degrees) at which light can be captured with an optical instrument. The AFOV is defined by the focal length of the lens and the size of the optical sensor. For instance, for the IS-based downlink $AFOV = 2 \times \arctan(h/2 \times f_{②})$ where h = 4.28 mm is the size of the image sensor.

Fig. 7(c) characterizes the misalignment tolerance of the system. The RoP is plotted as a function of vertical displacement for a fixed wireless link distance. The RoP for the PD-based uplink is −19.2 dBm when the system is fully aligned, while for the IS-based downlink is −20.2 dBm when the camera is displaced 50 mm in the vertical axis, i.e. the initial conditions of laboratory measurements, whose results were given in Section 3. For both VLC channels, we have two conditions: with pointing (i.e. both Tx and Rx are perfectly oriented) and without pointing. Given the configuration described in Section 2, the evaluation of the misalignment is carried out as follows.

For the PD-based uplink, the receiver (Rx_{PD}) is fixed, i.e., it has no offset, being the Tx_{PD} the one that is offset. The coverage area of the LED_{PD} conditions the RoP when no-pointing is performed (solid green line in Fig. 7(c)), when a pointing is performed (dashed green line in Fig. 7(c)), the RoP is conditioned by the FOV = 3.60 degrees, of the receiver. Since it does not depend on the coverage area, the RoP has a flat behavior up to around 47 mm, and decreases when the FOV of the receiver is smaller than the angle of incidence of the light emitted by the LED_{PD}. The minimum RoP required to transmit QPSK is −26.5 dBm corresponding to a misalignment of 37 mm with no-pointing (see Fig. 6(a)), whereas, with pointing, the same RoP corresponds to a 55 mm offset.

For the IS-based downlink, the transmitter (Tx_{IS}) is fixed, i.e., it has no offset, being the camera the one that has an offset. It is observed that the RoP decreases as we move further from the coverage area of the optical source. The differences in RoP due to pointing are related to the fact that the angle of incidence of the light emitted by the optical source is greater than the camera's AFOV = 2.45 degrees, i.e. it restricts the displacement to 32 mm, which coincides with the abrupt decrease of the optical power (solid red line) in Fig. 7(c). By proper pointing, the angle of relative incidence is reduced, thus losses are only due to the loss of coverage within the light cone (dashed red line).

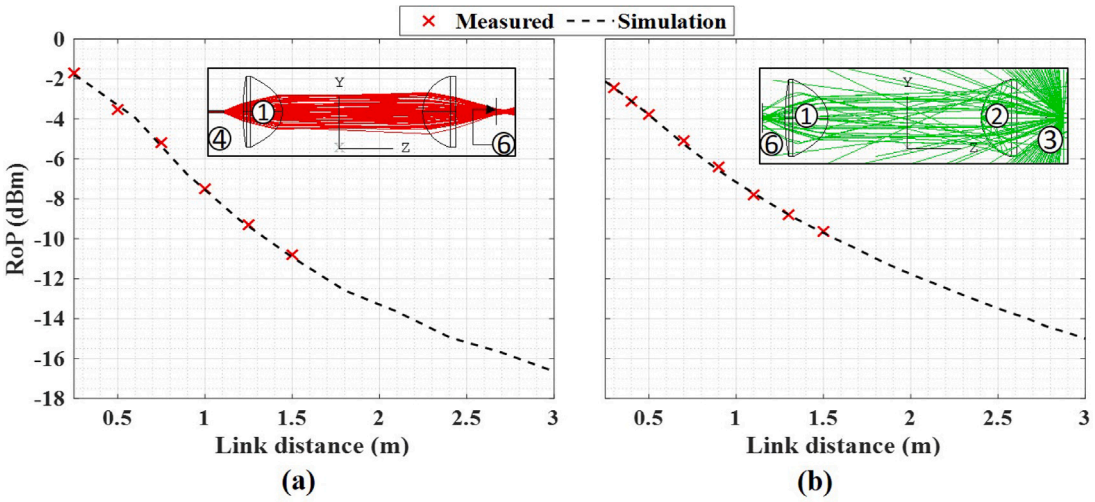

Fig. 8. Experimental (symbols) and simulated (dashed line) RoP vs. distance for: (a) IS-based wireless link; (b) PD-based wireless link. Insets show the workspace configuration layout in Zemax for both links.

A second simulation of the wireless optical channels is carried out to determine the channel propagation losses as a function of the link distance. To validate the simulation results first, we compared them with those obtained from laboratory measurements. Fig. 8 shows the simulated (dashed line) and measured (solid line with squares) RoP as a function of wireless link distance, both obtained with a 9.8 mm diameter S120C optical power sensor (see ⑥ in insets of Fig. 8). In the simulation, the workspace configuration is performed independently on each link replicating the laboratory setup (insets in Fig. 8). Note that both the experimental and simulated IS-based setup for power measurements employs a 25.3 mm focal lens before the power sensor. It can be observed that curves from simulations show very good agreement with measurements and allow to extend the RoP vs. link distance results.

Finally, Fig. 9 compares peak data rates of the PD-based uplink as a function of distance, i.e. 1.5–3.5 m range as appropriate for indoor applications, for different modulation formats and bandwidths. Such peak data rates were obtained by multiplying the maximum allowed bandwidth according to the EVM FEC threshold level in Fig. 6 by the number of bits per symbol. The simulations of the optical channel allowed to obtain the estimated distances for such RoP values. Note that in this case, the simulations, shown in the inset of Fig. 9, employ a 1 mm size detector to replicate the full link budget, as described in Table 2. RoP is -19.2 dBm for 1.5 m distance, which corresponds to the experimental results. For distances from 1.5 m to 2 m, it is observed that 16-QAM modulation format provides the highest data rate, i.e. 160 Mbps. For the received optical power after 1.5 m wireless link (-19.2 dBm), 64-QAM modulation has no superior performance to QPSK and 16-QAM. From -21.9 dBm and for lower values of RoP, corresponding to a wireless link distance larger than 1.9 m, QPSK is preferable over other modulation formats since it achieves higher throughput.

5. Conclusion

This paper demonstrates an asymmetric full-duplex hybrid VLC link that combines passive distribution of optical signals over POF and luminaire-free wireless connectivity. The system provides a passive point-to-point indoor access point using off-the-shelf components. The system includes a low-speed (kbps) IS-based channel as the downlink, and a high-speed (tens of Mbps) PD-based channel operating as the uplink.

The experimental results of the proposed system have been evaluated, presented and discussed in terms of EVM and SoR. For the PD-based uplink, rates of 160 Mbps using a 16-QAM modulation scheme and 120 Mbps using a QPSK and 64-QAM modulation schemes have been demonstrated for a RoP of -19.2 dBm over a 1.5 m optical wireless link. While for the IS-based downlink, a data rate of 500 bps with a SoR of 98.6% was achieved using an NRZ-OOK modulation format over the same wireless link distance. The effects of crosstalk in the system have been mitigated without the need of additional hardware components: the IS receiver makes use of a software RGB color filtering, meanwhile the PD receiver takes advantage of the directivity of the coupler to prevent saturation in the optical domain, whereas the use of different frequencies in the electrical domain allows the spectral separation of the signals in both links.

The experimental measurements have been complemented with simulations of the wireless links, which lead to an estimation of the misalignment tolerance in the PD-based uplink of 37 mm when there is no pointing between Tx and Rx while the tolerance increases to 55 mm with proper pointing. For the IS-based downlink, the AFOV of the camera restricts the misalignment to a maximum of 32 mm when there is no proper pointing. Finally, simulation results allow to provide the maximum experimental bit rates in terms of wireless distances, i.e. 10 MHz bandwidth QPSK signal (20 Mbps) can be transmitted up to 3.5 m link with a RoP of -26.5 dBm, while the IS-based system achieves a data rate of 500 bps with a SoR of 92.9% over 2.5 m and the SoR was 84.3% over 3.5 m.

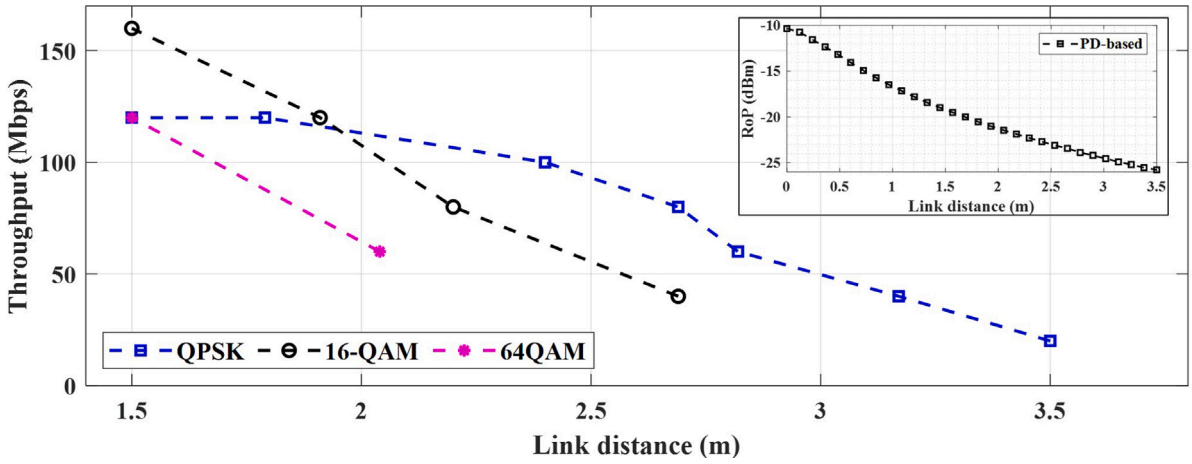

Fig. 9. Maximum high-speed channel throughput vs. link distance for different modulation formats.

Declaration of competing interest

The authors declare that they have no known competing financial interests or personal relationships that could have appeared to influence the work reported in this paper.

Data availability

Data will be made available on request.

Acknowledgments

This work was based upon work from COST Action CA19111 (European Network on Future Generation Optical Wireless Communication Technologies, NEWFOCUS), supported by COST (European Cooperation in Science and Technology), and also supported by MCIN/AEI/10.13039/501100011033 and ERDF A way of making Europe under Grant RTI2018-101658- B-I00 FOCAL, and also supported by the Czech Technical University in Prague under the CTU Global Postdoc Fellowship Program and TACR project FW01010571.

References

[1] Z. Ghassemlooy, L.N. Alves, S. Zvánovec, M.-A. Khalighi, Introduction, in: Visible Light Communications, Theory and Applications, CRC Press, 2017, pp. 1–8.
[2] S. Arnon, Visible Light Communication, in: Visible Light Communication, Cambridge University Press, 2015.
[3] S. Rajagopal, R.D. Roberts, S.K. Lim, IEEE 802.15.7 visible light communication: Modulation schemes and dimming support, IEEE Commun. Mag. 50 (3) (2012) 72–82.
[4] A. Aliaberi, P.C. Sofotasios, S. Muhaidat, Modulation schemes for visible light communications, in: 2019 International Conference on Advanced Communication Technologies and Networking (CommNet), 2019, pp. 1–10.
[5] K. Lee, H. Park, Channel model and modulation schemes for visible light communications, in: Midwest Symposium on Circuits and Systems, Vol. 00, IEEE, 2011, pp. 26–29.
[6] M.B. Rahaim, T. Little, Toward practical integration of dual-use VLC within 5G networks, IEEE Wirel. Commun. 22 (4) (2015) 97–103.
[7] F. Wang, Y. Liu, F. Jiang, N. Chi, High speed underwater visible light communication system based on LED employing maximum ratio combination with multi-PIN reception, Opt. Commun. 425 (December 2017) (2018) 106–112.
[8] I. Takai, T. Harada, M. Andoh, K. Yasutomi, K. Kagawa, S. Kawahito, Optical vehicle-to-vehicle communication system using LED transmitter and camera receiver, IEEE Photonics J. 6 (5) (2014) 1–14.
[9] H. Binti Che Wook, T. Komine, S. Haruyama, M. Nakagawa, Visible light communication with LED-based traffic lights using 2-dimensional image sensor, in: CCNC 2006. 2006 3rd IEEE Consumer Communications and Networking Conference, 2006. Vol. 1, 2006, pp. 243–247.
[10] M. Joncic, R. Kruglov, M. Haupt, R. Caspary, J. Vinogradov, U.H.P. Fischer, Four-channel WDM transmission over 50-m SI-POF at 14.77 Gb/s using DMT modulation, IEEE Photonics Technol. Lett. 26 (13) (2014) 1328–1331.
[11] W.O. Popoola, E. Pikasis, I. Osahon, Hybrid polymer optical fibre and visible light communication link for in-home network, in: 2017 26th Wireless and Optical Communication Conference, WOCC 2017, no. Mc, IEEE, 2017, pp. 2–7.
[12] I.N. Osahon, E. Pikasis, S. Rajbhandari, W.O. Popoola, Hybrid POF/VLC link with M-PAM and MLP equaliser, in: 2017 IEEE International Conference on Communications, ICC, IEEE, 2017, pp. 1–6.
[13] IEEE Standard for Local and Metropolitan Area Networks–Part 15.7: Short-Range Optical Wireless Communications, IEEE Std 802.15.7-2018 (Revision of IEEE Std 802.15.7-2011), 2019, pp. 1–407.

[14] X. Liu, X. Wei, L. Guo, DIMLOC: Enabling high-precision visible light localization under dimmable LEDs in smart buildings, IEEE Internet Things J. 6 (2) (2019) 3912–3924.
[15] T. Yamazato, I. Takai, H. Okada, T. Fujii, T. Yendo, S. Arai, M. Andoh, T. Harada, K. Yasutomi, K. Kagawa, S. Kawahito, Image-sensor-based visible light communication for automotive applications, IEEE Commun. Mag. 52 (7) (2014) 88–97.
[16] Z. Ghassemlooy, P. Luo, S. Zvanovec, Optical camera communications, in: M. Uysal, C. Capsoni, Z. Ghassemlooy, A. Boucouvalas, E. Udvary (Eds.), Optical Wireless Communications: An Emerging Technology, Springer International Publishing, Cham, 2016, pp. 547–568.
[17] T. Le, N.-T. Le, Y.M. Jang, Performance of rolling shutter and global shutter camera in optical camera communications, in: 2015 International Conference on Information and Communication Technology Convergence, ICTC, 2015, pp. 124–128.
[18] E. Sisinni, A. Saifullah, S. Han, U. Jennehag, M. Gidlund, Industrial internet of things: Challenges, opportunities, and directions, IEEE Trans. Ind. Inform. 14 (11) (2018) 4724–4734.
[19] D. O'Brien, H. Le Minh, L. Zeng, G. Faulkner, K. Lee, D. Jung, Y. Oh, E.T. Won, Indoor Visible Light Communications: Challenges and Prospects, 2008, 709106.
[20] C. Chen, S. Fu, X. Jian, M. Liu, X. Deng, Z. Ding, NOMA for energy-efficient lifi-enabled bidirectional IoT communication, IEEE Trans. Commun. 69 (3) (2021) 1693–1706.
[21] H. Jung, S.M. Kim, A full-duplex LED-to-LED visible light communication system, Electronics (Switzerland) 9 (10) (2020) 1–10.
[22] Q. Chen, D. Han, M. Zhang, Z. Ghassemlooy, A.C. Boucouvalas, Z. Zhang, T. Li, X. Jiang, Design and demonstration of a TDD-based central-coordinated resource-reserved multiple access (CRMA) scheme for bidirectional VLC networking, IEEE Access 9 (2021) 7856–7868.
[23] C. Ribeiro Barbio Corrêa, K.A. Mekonnen, F. Huijskens, T. Koonen, E. Tangdiongga, Passive OFE multi-Gbps VLC transmission using POF as a feeder line, Microw. Opt. Technol. Lett. (2022).
[24] E. Eso, S. Teli, N.B. Hassan, S. Vitek, Z. Ghassemlooy, S. Zvanovec, 400 M rolling-shutter-based optical camera communications link, Opt. Lett. 45 (5) (2020) 1059–1062.
[25] Y. Liu, Decoding mobile-phone image sensor rolling shutter effect for visible light communications, Opt. Eng. 55 (1) (2016) 016103.
[26] J.A. Apolo, B. Ortega, V. Almenar, Hybrid POF/VLC links based on a single LED for indoor communications, Photonics 8 (7) (2021).
[27] R. Schmogrow, B. Nebendahl, M. Winter, A. Josten, D. Hillerkuss, S. Koenig, J. Meyer, M. Dreschmann, M. Huebner, C. Koos, J. Becker, W. Freude, J. Leuthold, Error vector magnitude as a performance measure for advanced modulation formats, IEEE Photonics Technol. Lett. 24 (1) (2012) 61–63.
[28] International Telecommunication Union, Forward error correction for high bit-rate DWDM submarine systems, in: ITU-T Recommendation G.975.1, 2004.

Juan A. Apolo received the bachelor's. degree in Electronics and Telecommunications Engineering from Universidad Técnica Particular de Loja (Ecuador) in 2018; during these years, he registered three national patents related to IoT. In 2020 he received the M.Sc. degree in telecommunication technologies, systems, and networks from Universitat Politècnica de València (UPV), Spain, Where he is currently a Ph.D. student with the Photonics Research Labs, Institute of Telecommunications and Multimedia Applications. His research is focused on free space optics and visible light communications.

Dr. Shivani Rajendra Teli received her Ph.D. in 2021 within visible light-based interoperability and networking (ViSIoN) which is a project under European Union's Horizon H2020 Marie Skłodowska-Curie Innovative Training Network (MSCA ITN) from the Faculty of Electrical Engineering, Czech Technical University (CTU) in Prague. She is currently working as a PostDoc Researcher within CTU Global Fellowship program. She received her M. Sc. degree from Department of Information and Communications Engineering, Pukyong National University, Busan, Korea and Bachelor's degree from Savitribai Phule Pune University, Maharashtra, India, in 2018 and 2015, respectively. Her research interests are wireless communication systems, visible light communications and optical camera communications for Internet of things and sensor networks.

Carlos Guerra-Yanez received his M.Eng. degree in 2021 from Universidad de Las Palmas de Gran Canaria, Spain. He is currently a Ph.D. student at the Wireless and Fiber Optics group at Czech Technical University in Prague, Czech Republic. His current research interests include signal processing, modulation techniques, and channel coding for visible light communications as well as quantum key distribution over free-space optics.

Vicenç Almenar received the Telecomunications Engineering and Ph.D. degrees from the Universitat Politècnica de València (UPV), Valencia, Spain, in 1993 and 1999, respectively. In 1993, he joined the Communications Department, UPV, became Associate Professor in 2002 and Full Professor in 2017. He was Deputy Director of the Department from 2004 until 2014. His current research interests include OFDM, MIMO, and signal processing techniques for wireless and optical communications systems.

Beatriz Ortega (Member, IEEE) received the M.Sc. degree in physics from the Universidad de Valencia, in 1995, and the Ph.D. degree in telecommunications engineering from the Universidad Politécnica de Valencia, in 1999. She currently works with the Departamento de Comunicaciones, Universitat Politècnica de València, where she also holds a Full Professorship since 2009 and collaborates as a Group Leader with the Photonics Research Labs, Institute of Telecommunications and Multimedia Applications. She has published more than 200 articles and conference contributions in fiber Bragg gratings, microwave photonics, and optical networks. She has held several patents and is also a co-founder of EPHOOX company. She has participated in a large number of European Networks of Excellence and Research and Development projects and other national ones. Her main research interests include optical devices, optical networks, and microwave photonic systems and applications.

Stanislav Zvanovec (Senior Member, IEEE) received the M.Sc. and Ph.D. degrees from the Faculty of Electrical Engineering, Czech Technical University (CTU) in Prague, Prague, Czechia, in 2002 and 2006, respectively. He currently works as a Full Professor and the Deputy Head of the Department of Electromagnetic Field and the Chairperson of Ph.D. branch with CTU in Prague. He has authored two books and coauthored the recent book Visible Light Communications: Theory and Applications, several book chapters, and more than 250 journal and conference papers. His current research interests include free space optical and fiber optical systems, visible-light communications, OLED, RF over optics, and electromagnetic wave propagation issues for millimeter-wave band.